Using DNA to construct and power a nanoactuator

Friedrich C. Simmel and Bernard Yurke
Bell Laboratories, Lucent Technologies, Murray Hill, New Jersey 07974
(Received 31 August 2000; revised manuscript received 11 January 2001; published 29 March 2001)

A DNA-based molecular machine is described which has two movable arms that are pushed apart when a strand of DNA, the fuel strand, hybridizes with a single-stranded region of the molecular machine. Through the process of branch migration, a second strand of DNA complementary to the fuel strand is able to remove the fuel strand from the molecular machine, restoring it to its original configuration. Compared with the molecular tweezers we had previously devised, this machine, which we call a nanoactuator, has a reduced tendency to form dimers.

DOI: 10.1103/PhysRevE.63.041913 PACS number(s): 87.14.Gg, 87.16.Nn, 07.10.Cm

Understanding the mechanisms by which directed motion can be induced on a molecular scale is an active area of research [1]. Much of this work has been driven by a desire to understand how biological molecular motors operate and most of this work has focused on thermal ratchets [2]. Experimental systems exhibiting thermal ratchet behavior have been devised [3]. More recently several single-molecule devices exhibiting directed motion have been made [4,5]. A DNA-based molecular motor, driven by hybridization energy, has been reported by us [6]. Because of the potential application to nanotechnology, it is desirable to explore various ways of constructing molecular-scale engines. Here a DNA-based engine is described in which a pushing force rather than a pulling force is generated during the power stroke.

DNA has proved to be a versatile material from which to construct nanoscale structures [7] and machines. This versatility results primarily from its simple molecular recognition chemistry: Two strands of single-stranded (ss) DNA hybridize well to form double-stranded (ds) DNA only if the sequences of bases of the two strands are complementary [8]. The large size of the combinatorial space [9] of nucleotide sequences that can be used as labels to determine which strands of DNA hybridize with each other facilitates the construction of complex structures. This has allowed the assembly of a variety of wire frame polyhedral structures [10], complex knots [11], and two-dimensional sheets consisting of DNA tiles [12]. This may form the basis for a versatile self-assembly technology [13]. Also, through molecular selection experiments various DNA structures have been found that are capable of enzymatic activity [14]. Progress has also been made in the rational design of DNA-based molecular machines [6,15]. In one machine [15] the *B-Z* transition of DNA was used to produce structural rearrangements. More recently we have used DNA hybridization to power the closure of a tweezerslike DNA structure [6]. A means for reopening these molecular tweezers was provided by utilizing the branch migration process whereby one strand of DNA can displace another as each competes for binding with a third complementary strand [16]. A related molecular machine is reported here. We refer to this engine as a nanoactuator. In this machine DNA hybridization is used to push two components apart rather than to pull them together. In addition, the nanoactuator is less susceptible to dimer formation than are the molecular tweezers.

The nucleotide sequences for the strands of DNA used to construct and operate the actuator are given in Table I. The device and its operation are illustrated in Fig. 1. As shown in Fig. 1(a), the molecular machine is constructed from two strands of DNA labeled *A* and *B* that hybridize to form a loop with two 18-base-pair double-stranded regions. Since the persistence length [20] of dsDNA, ~ 50 nm, is much longer than the length of these overlap regions, the double-stranded regions serve as rigid arms. Since ssDNA has a short persistence length [21], the four-base region of *A* that remains single stranded, H_A of Table I, serves as a flexible hinge between the two arms. The 48-base region of *B* that remains single stranded consists of a 40-base region, *M* of Table I, which we refer to as the motor domain. The motor domain is sandwiched between the two four-base regions S_{B1} and S_{B2} that serve as spacers. Thermally driven fluctuations of the single-stranded portion of *B* give rise to entropic forces that pull the two arms toward each other. Hence, in its relaxed configuration there will be a mean angle of separation between the two arms that is less than that which would be obtained if the single-stranded region of *B* were pulled straight.

As shown in Fig. 1(b), the fuel strand *F* is used to push the two arms apart into the straightened configuration. As

TABLE I. Oligonucleotide sequences. The 5′ end of each sequence is at the left. An overbar denotes the complement of an oligonucleotide sequence.

$A = A_1\ H_A\ A_2$	$B = \overline{A_1}\ S_{B1}\ M\ S_{B2}\ \overline{A_2}$
$\alpha = \alpha_1\ \mathrm{H}_\alpha\ \alpha_2$	$\beta = \overline{\alpha_1}\ S_{B1}\ M\ S_{B2}\ \overline{\alpha_2}$
$\beta_{12} = \overline{A_1}\ S_{B1}\ M\ S_{B2}\ \overline{\alpha_2}$	$\beta_{21} = \overline{\alpha_1}\ S_{B1}\ M\ S_{B2}\ \overline{A_2}$
$\mathrm{F} = \overline{M}\ \tau$	$\tau = \mathrm{TGCTACGA}$
$H_A = \mathrm{ATCA}$	$H_\alpha = \mathrm{ATTT}$
$S_{B1} = \mathrm{CTGG}$	$S_{B2} = \mathrm{AACG}$
$A_1 = \mathrm{TGCCTTGTAAGAGCGACC}$	
$A_2 = \mathrm{ACCTGGAATGCTTCGGAT}$	
$\alpha_1 = \mathrm{GCGATGAAGTGTCCACCT}$	
$\alpha_2 = \mathrm{CCGTATGGAGCAGAATCC}$	
$M = \mathrm{TAACAATCACGGTCTATGCG}$	
GGAGTCCTACTGTCTGAACT	

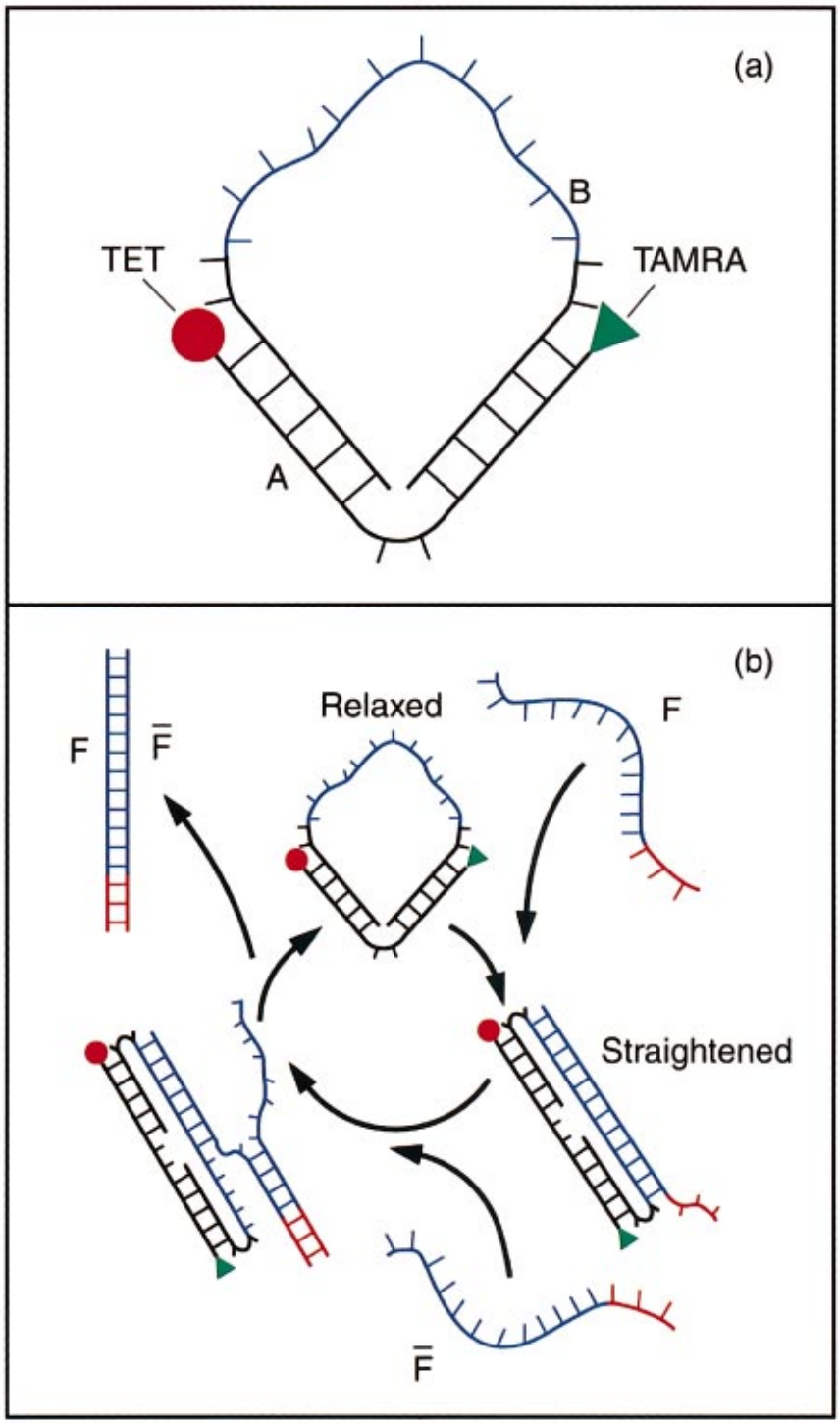

FIG. 1. (Color) The nanoactuator (a) consists of two strands of DNA labeled *A* and *B* that hybridize together into a looplike structure consisting of two stiff double-stranded arms held together by a short and a long single-stranded region. The operation of the nanoactuator is shown in (b). Upon hybridizing with the actuator, the fuel strand pushes the arms apart into a ''straightened'' configuration. The complement of *F*, denoted by $\overline{F}$, removes *F* from the actuator through strand displacement by branch migration. A double-stranded waste product, *F* hybridized with $\overline{F}$, is produced each time the actuator is cycled between its ''relaxed'' and straightened states.

indicated in Table I, *F* possesses a region $\overline{M}$ that is complementary to the motor domain of *B*. The hybridization of this region of *F* with the *B* strand pushes the two arms apart. From the average free energy change associated with the hybridization of a complementary base pair (-78 meV at 20 °C) and the separation between bases in dsDNA (0.34 nm), one estimates that pushing forces of order 37 pN could be developed. This is respectable even for biological molecular motors. It is comparable to the stall force generated by RNA polymerase [17], the most powerful ATPase molecular motor known [18], and to the forces generated by actin and microtubule polymerization [19]. The magnitude of the force applied to an actuator arm is smaller than this number by a factor of 2 or more due to mechanical advantage factors. On hybridizing with the motor domain of *B*, a single-stranded region of *F*, called the toehold (τ in Table I), remains. The actuator is restored to its initial configuration by the introduction of the complement $\overline{F}$ of the fuel strand. This strand first attaches itself to the fuel strand via the toehold. $\overline{F}$ then competes with the actuator for binding with the fuel strand

through branch migration [16]. This is a random walk process associated with the temporary breaking of base pair bonds by thermal fluctuations. The mean time between steps is on the order of 10 μs. The random walk makes a first passage to the point where F and $\overline{F}$ are fully hybridized. At this point the actuator has been restored to its relaxed configuration and the waste product of F fully hybridized with $\overline{F}$ has been created. By successively adding F and then $\overline{F}$ the actuator can be repeatedly cycled between its straightened and relaxed configurations.

All oligomers used in the experiments reported here were purchased and purified, as in [6], by Integrated DNA Technologies, Inc. (IDT). Stock solutions were prepared by resuspending the lyophilized oligonucleotides in TE buffer [10 mM Tris (tris(hydroxymethyl)-aminomethane) pH 8.0, 1 mM EDTA (ethylene diamine tetra acetic acid)] at a nominal 25 μM concentration. Unless stated otherwise, experiments were performed at 1 μM concentrations at 20 °C, by adding DNA stock to a 48 μl volume of sodium phosphate/sodium chloride (SPSC) buffer (pH 6.5, 1M NaCl).

Gel electrophoresis experiments supplementing those in [6] were performed to demonstrate that there is no unexpected hybridization between any two of the strands A, B, F, $\overline{F}$, and their subsections. This indicates that only those sections of the strands A, B, F, and $\overline{F}$ that were designed to hybridize with each other do, and hence the interaction between the strands are those depicted in Fig. 1.

Strand A was labeled at the 5′ and 3′ ends with the dyes TET and TAMRA, respectively. Fluorescence resonance energy transfer (FRET) [22] between these two dyes was used to monitor the separation between the two arms of the actuator. The TET dye was excited with 514.5 nm argon ion laser light, and the fluorescence was measured as described in Ref. [6]. The degree of fluorescence quenching as a function of dye separation had been previously determined [6]. Titration experiments using the TET fluorescence as an indicator were performed to determine stoichiometry between the stock solutions of various DNA strands.

When strand B is added to strand A in stoichiometric amounts the TET fluorescence increases by a factor of 2.3. When strand F is added to this the fluorescence increases by another factor of 1.8. From this it is inferred that the distance between the two dyes when the actuator is in its relaxed configuration is 5.1 nm. In the straightened configuration the distance between the two dyes is $\sim$13 nm. Figure 2 shows a plot of fluorescence with time as the actuator is cycled between its relaxed configuration and its straightened configuration through successive applications of F and $\overline{F}$. Under our experimental conditions, the time for half completion of the straightening reaction is 21 s while the time for half completion of the relaxation reaction is 59 s. The decay in fluorescence is fully accounted for by the decrease in the actuator concentration that results from successive addition of 3.0 μl F and 3.1 μl $\overline{F}$ at nominal 12.5 μM concentration. To demonstrate that the observed TET fluorescence changes are primarily due to FRET with the TAMRA dye, actuators were constructed in which the A strand was only TET labeled. For these strands a 10% fluorescence change was noted during hybridization with B. No further fluorescence change, apart from that due to dilution, was detected upon operating these actuators.

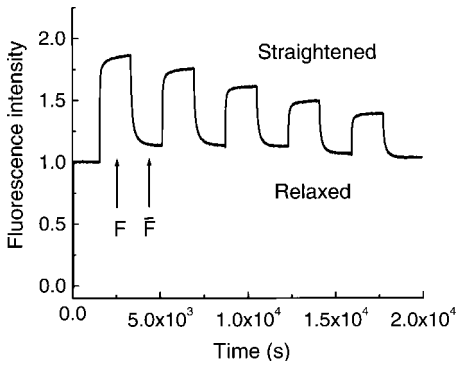

FIG. 2. The fluorescence intensity as a function of time as the actuator is successively straightened and relaxed. When F is added, the fluorescence increases due to the increased distance between the TET and TAMRA dyes. When $\overline{F}$ is added the fluorescence decreases.

A correctly formed actuator consists of a single A and a single B strand hybridized together. More complex structures consisting of loops possessing two or more A strands and B strands can form. At the concentrations employed in our experiments the smallest of these unwanted loops dominate and, hence, we will refer to these structures as dimers and to correctly assembled actuators as monomers. To quantitate the formation of dimers, a second actuator was designed using the sequences α and β instead of A and B. Strands A and α can combine with the strands B and β, respectively, to form actuators or they can be cross linked using the strands β_{12} and β_{21}. The latter sequences are both partly complementary to sections of A and α (cf. Table I). Hence, the smallest looplike structure formed by the hybridization of stoichiometric amounts of A, α, β_{12}, and β_{21} is of the same size as the simplest dimer formed by two A (α) strands with two B (β) strands.

The amount of dimer formation was assessed in two different ways. The first method employed polyacrylamide gel electrophoresis (PAGE). Figure 3 shows the result of a PAGE run, in which the nanoactuator is compared with the dimer standard formed by A, α, β_{12}, and β_{21}. The run was performed under nondenaturing conditions at 20 °C and with a constant current of $I=20$ mA, using a 5% polyacrylamide gel and TBE (Tris-borate-EDTA, pH 8.3) as reservoir buffer. Prior to loading the gel, reactions were performed with equal amounts (25 pmol) of dye-labeled strands to which stoichiometric amounts of all other strands were added, yielding a typical final concentration of 5 μM for each species. Each reaction step was given a minimum of 10 min to proceed to near completion. The PAGE experiment confirms that little dimer formation takes place (see caption Fig. 3).

The second method of checking for large loop formation employed a series of fluorescence measurements ($F1$–$F4$), summarized in Table II. These experiments were carried out at concentrations and buffer conditions as in the measurements for Fig. 2. The total DNA concentration was the same

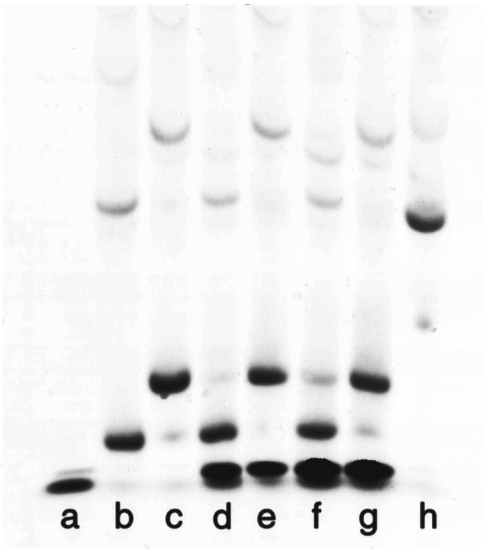

FIG. 3. Test of dimer formation using polyacrylamide gel electrophoresis: DNA migrates from top to bottom; shorter strands migrate faster. In lanes (a)–(g) the actuator is assembled and operated, whereas lane (h) contains the dimer construct made from A, α, β_{12}, and β_{21} as described in the text. Lane (a) contains strand A. Lane (b) shows the result of the assembly of actuators from strands A and B. The lowest and darkest band corresponds to the correctly assembled device, whereas the higher and fainter bands are due to dimers, as can be judged from comparison with lane (h). In (c) the actuator is straightened by adding the fuel strand F. The dark actuator band shifts accordingly to higher molecular weight. The dimer ''ladder'' also shifts, as F can also bind to dimers. The faint band at the height of the relaxed actuator is due to a slight deviation from stoichiometric conditions. In lanes (d)–(g) the actuator is relaxed and straightened twice by successively adding the removal strand $\bar{F}$ and the fuel strand F. Actuators and dimers shift accordingly. As errors in stoichiometry accumulate over several cycles, faint bands appear ''out of phase.'' The dark bands at the bottom of lanes (d)–(g) are produced by the ''waste product'' $F\bar{F}$.

for all four experiments and all strands were mixed in stoichiometry. Where two strands of a given type were used, such as A and α in $F2$, A and $\tilde{A}$ in $F3$, and $\tilde{A}$ and α in $F4$, 1:1 mixtures were employed. Table II contains a set of four equations for the eight variables x, I_A, $I_{\tilde{A}}$, $I_{A,A}$, $I_{A,\alpha}$, $I_{A,\tilde{A}}$, $I_{\tilde{A},\tilde{A}}$, $I_{\tilde{A},\alpha}$. This system can be solved under the following assumptions. (i) All fully dye-labeled dimers exhibit the same fluorescence ($I_{A,A}=I_{A,\alpha}$). (ii) The fluorescence of dimers formed by A and unlabeled $\tilde{A}$ and that of dimers composed of α and $\tilde{A}$ is equal ($I_{A,\tilde{A}}=I_{\tilde{A},\alpha}$). When A was substituted by $\tilde{A}$ in $F1$ the fluorescence was less than 0.5% of that observed without the substitution and was consistent with zero, indicating that (iii) $I_{\tilde{A}}=I_{\tilde{A},\tilde{A}}=0$. This reduces the number of unknown variables to four and the solution of the system of equations in Table II is

TABLE II. Experiments $F1$–$F4$ performed to determine the amount of dimer formation during the actuator assembly. A, B, α, β_{12}, and β_{21} are ssDNA strands specified in Table I. A and α are both TET and TAMRA labeled; strand $\tilde{A}$ has the same sequence as A, but is not fluorescently labeled. The first column of the table lists the strands used for the experiments. By construction, in $F2$ and $F4$ only dimers can form, whereas in $F1$ and $F3$ a mixture of correctly assembled actuators and dimers can be expected. In the second column this is expressed in terms of the fluorescence intensities of the reaction mixtures after completion of the assembly reaction. The fluorescence contributions of correctly assembled actuators are termed I_A and $I_{\tilde{A}}$. The other contributions $I_{A,A}$, $I_{A,\alpha}$, $I_{A,\tilde{A}}$, $I_{\tilde{A},\tilde{A}}$, and $I_{\tilde{A},\alpha}$ stem from dimers formed by the strands listed in the subscripts. $x\in[0,1]$ is the amount of dimer formation, to be determined by this set of experiments. The final column contains the actually measured fluorescence intensities I normalized to the final fluorescence value I_{F1} for experiment $F1$.

	Strands	Final fluorescence I	I/I_{F1}
$F1$	A,B	$I_{F1}=xI_A+\frac{1}{2}(1-x)I_{A,A}$	1
$F2$	$A,\alpha,\beta_{12},\beta_{21}$	$I_{F2}=I_{A,\alpha}/2$	0.822
$F3$	$A,\tilde{A},B$	$I_{F3}=(x/2)I_A+(x/2)I_{\tilde{A}}$ $+(1-x)I_{A,A}/8$ $+(1-x)I_{A,\tilde{A}}/4$ $+(1-x)I_{\tilde{A},\tilde{A}}/8$	0.515
$F4$	$\tilde{A},\alpha,\beta_{12},\beta_{21}$	$I_{F4}=I_{\tilde{A},\alpha}/2$	0.696

$$x=1-(4I_{F3}-2I_{F1})/(2I_{F4}-I_{F2}), \tag{1}$$

where x is the fraction of correctly assembled actuators. Inserting the experimental values for I_{F1}, I_{F2}, I_{F3}, and I_{F4}, one finds that 90% of the DNA strands are assembled properly. In contrast to the molecular tweezers [6], the dimer formation takes place during the assembly of the molecular machine and not during its operation. Thus, in principle one could purify the actuators after the assembly step and operate exclusively with correctly assembled devices.

In conclusion, we have constructed a DNA-based actuator that can be cycled between a relaxed and a straightened state. Like the molecular tweezers, it is a clocked molecular motor operated by successive addition of fuel strands followed by their complements. Unlike the molecular tweezers, hybridization of the fuel strand with the actuator pushes the two arms apart. Also, because of its loop structure, the actuator is less susceptible to forming dimers than are the molecular tweezers.

F.C.S. thanks the Alexander von Humboldt Foundation for support through the Feodor Lynen program.

[1] M. Porto, M. Urbakh, and J. Klafter, Phys. Rev. Lett. **85**, 491 (2000); , **84**, 6058 (2000); A. W. Ghosh and S. V. Khare, *ibid.* **84**, 5243 (2000); I. Derényi, M. Bier, and R. D. Astumian, *ibid.* **83**, 903 (1999); H. Qian, *ibid.* **81**, 3063 (1998); T. Harms and R. Lipowsky, *ibid.* **79**, 2895 (1997); F. Jülicher and J. Prost, *ibid.* **78**, 4510 (1997); **75**, 2618 (1995).
[2] M. O. Magnasco, Phys. Rev. Lett. **71**, 1477 (1993); R. D. Astumian and M. Bier, *ibid.* **72**, 1766 (1994).
[3] L. P. Faucheux *et al.*, Phys. Rev. Lett. **74**, 1504 (1995); J. Rousselet *et al.*, Nature (London) **370**, 446 (1994); C. Mennerat-Robilliard *et al.*, Phys. Rev. Lett. **82**, 851 (1999).
[4] T. R. Kelly, H. De Silva, and R. A. Silva, Nature (London) **401**, 150 (1999).
[5] N. Koumura *et al.*, Nature (London) **401**, 152 (1999).
[6] B. Yurke *et al.*, Nature (London) **406**, 605 (2000).
[7] N. C. Seeman, Acc. Chem. Res. **30**, 357 (1997); C. M. Niemeyer, Angew. Chem. Int. Ed. Engl. **36**, 585 (1997).
[8] J. SantaLucia, Jr., H. T. Allawi, and P. A. Seneviratne, Biochemistry **35**, 3555 (1996).
[9] R. Deaton *et al.*, Phys. Rev. Lett. **80**, 417 (1998).
[10] J. Chen and N. C. Seeman, Nature (London) **350**, 631 (1991).
[11] C. Mao, W. Sun, and N. C. Seeman, Nature (London) **386**, 137 (1997).
[12] E. Winfree *et al.*, Nature (London) **394**, 539 (1998).
[13] C. A. Mirkin *et al.*, Nature (London) **382**, 607 (1996); A. P. Alivisatos *et al.*, *ibid.* **382**, 609 (1996); E. Braun *et al.*, *ibid.* **391**, 775 (1998).
[14] G. F. Joyce, Proc. Natl. Acad. Sci. U.S.A. **95**, 5845 (1998); R. R. Breaker, Nat. Biotechnol. **15**, 427–431 (1997).
[15] C. Mao *et al.*, Nature (London) **397**, 144 (1999).
[16] C. Green and C. Tibbetts, Nucleic Acids Res. **9**, 1905 (1981).
[17] M. D. Wang *et al.*, Science **282**, 902 (1998).
[18] H.-Y. Wang *et al.*, Biophys. J. **74**, 1186 (1998).
[19] L. Mahadevan and P. Matsudaira, Science **288**, 95 (2000).
[20] S. B. Smith, L. Finzi, and C. Bustamante, Science **258**, 1122 (1992).
[21] S. B. Smith, Y. Cui, and C. Bustamante, Science **271**, 795 (1996); B. Tinland *et al.*, Macromolecules **30**, 5763 (1997).
[22] L. E. Morrison and L. M. Stols, Biochemistry **32**, 3095 (1993).